

## Article

# Green Concrete Based on Quaternary Binders with Significant Reduced of CO<sub>2</sub> Emissions

Grzegorz Ludwik Golewski 

Department of Structural Engineering, Faculty of Civil Engineering and Architecture, Lublin University of Technology, Nadbystrzycka 40 Str., 20-618 Lublin, Poland; g.golewski@pollub.pl; Tel.: +48-81-538-4394

**Abstract:** The article presents studies of plain concretes prepared based on a quaternary binder containing various percentages of selected supplementary cementitious materials (SCMs). The possibilities of nanotechnology in concrete technology were also used. An additional important environmental goal of the proposed solution was to create the possibility of reducing CO<sub>2</sub> emissions and the carbon footprint generated during the production of ordinary Portland cement (OPC). As the main substitute for the OPC, siliceous fly ash (FA) was used. Moreover, silica fume (SF) and nanosilica (nS) were also used. During examinations, the main mechanical properties of composites, i.e., compressive strength ( $f_{cm}$ ) and splitting tensile strength ( $f_{ctm}$ ), were assessed. The microstructure of these materials was also analyzed using a scanning electron microscope (SEM). In addition to the experimental research, simulations of the possible reduction of CO<sub>2</sub> emissions to the atmosphere, as a result of the proposed solutions, were also carried out. It was found that the quaternary concrete is characterized by a well-developed structure and has high values of mechanical parameters. Furthermore, the use of green concrete based on quaternary binders enables a significant reduction in CO<sub>2</sub> emissions. Therefore quaternary green concrete containing SCMs could be a useful alternative to plain concretes covering both the technical and environmental aspects. The present study indicates that quaternary binders can perform better than OPC as far as mechanical properties and microstructures are concerned. Therefore they can be used during the production of durable concretes used to perform structures in traditional and industrial construction.

**Keywords:** green concrete; quaternary binder; siliceous fly ash (FA); silica fume (SF); nanosilica (nS); SCMs; mechanical properties; microstructure; C-S-H phase; reduction of CO<sub>2</sub> emission



**Citation:** Golewski, G.L. Green Concrete Based on Quaternary Binders with Significant Reduced of CO<sub>2</sub> Emissions. *Energies* **2021**, *14*, 4558. <https://doi.org/10.3390/en14154558>

Academic Editors: Prodip K. Das, Sara Walker and Nigel D. Browning

Received: 2 July 2021  
Accepted: 25 July 2021  
Published: 28 July 2021

**Publisher's Note:** MDPI stays neutral with regard to jurisdictional claims in published maps and institutional affiliations.



**Copyright:** © 2021 by the author. Licensee MDPI, Basel, Switzerland. This article is an open access article distributed under the terms and conditions of the Creative Commons Attribution (CC BY) license (<https://creativecommons.org/licenses/by/4.0/>).

## 1. Introduction

For many years, the cement and concrete industry has faced a number of challenges, which include, among other things, the depletion of fossil fuel reserves, constant shortage of raw materials for production of composites, or abnormal growth in demand for this type of construction material, i.e., the concrete. Among the many problems associated with the production of concrete using traditional methods, concerns are also focused in terms of its negative impact on the natural environment. Counteracting climate change is currently one of the most important elements of world politics, e.g., [1].

Therefore, practically all environmental aspects of concrete structures are considered in the following three categories, e.g., [2–18]:

- consumption of natural resources;
- consumption of energy;
- CO<sub>2</sub> emission.

Unfortunately, the production of ordinary concrete in its traditional form has a negative reflection practically in all of the fields listed above. Manufacturing of concrete consumes a huge quantity of natural resources, mainly for the preparation of raw materials to burnout of Portland clinker, but also as an aggregate for concrete [19–21]. In addition, the production of ordinary Portland cement (OPC) involves considerable energy consumption,

both thermal and electrical [22–24], and evident air pollution by greenhouse gas (GHG) emission [25–28].

Nowadays, the most attention is paid to the greenhouse effect, to which the emission of CO<sub>2</sub> largely contributes. It covers approximately 55% of all GHG emissions. Because human activity increases the concentration of GHG in the atmosphere (mainly CO<sub>2</sub>) that hinder the emission of heat into outer space, thereby causing dangerous climate change, so in the field of pro-ecological activities, there are, among other things, intense efforts to reduce as much as possible emission of this harmful oxide [29–31].

It should be noted that currently, in almost all industry sectors, efforts are observed to quantify GHG emission, which allows identification of factors and production stages that pollute the environment the most. Such activities are undoubtedly the first step towards the implementation of solutions reducing their emission. Regarding the production of concrete it should be added that the CO<sub>2</sub> emission in this process concerns mainly burning the Portland clinker, which is necessary for the production of OPC, e.g., [32–34]. This problem will be further discussed in Section 2.

One of the options for reducing emissions of CO<sub>2</sub> produced in the processes of preparation of the main binder, i.e., OPC, there is limiting the share of clinker cement in its composition in favor of other useful materials. According to the assumptions, production of low-emission cement would be possible by lowering the clinker/cement ratio to a level of 0.7, which is expected in 2050. Currently, although this rate is gradually declining, it is still clearly disadvantageous. In the year 2000, the rate was 1.06, while currently has a value of 0.9 (Table 1). This value, although not as high as several decades ago, still does not correspond to the trends based on green technologies in the cement industry [35–40]. This is confirmed by the latest data on the production of OPC and Portland clinker in states with the largest global share, and the global average in this industry, which are summarized in Table 1 [41].

**Table 1.** World production of cement and clinker in 2019 [41].

Country	Production of Cement (mln ton)	Share(%)	Production of Clinker (mln ton)	Share(%)	Clinker/Cement Ratio
China	2200	53.7	1970	53.2	0.90
India	320	7.8	280	7.6	0.88
Vietnam	95	2.3	90	2.4	0.95
United States	89	2.2	103	2.8	1.16
Egypt	76	1.9	48	1.3	0.63
Indonesia	74	1.8	78	2.1	1.05
Iran	60	1.5	81	2.2	1.35
Russia	57	1.4	80	2.2	1.40
Republic of Korea	55	1.3	50	1.4	0.91
Brazil	55	1.3	60	1.6	1.09
Japan	54	1.3	53	1.4	0.98
Turkey	51	1.2	92	2.5	1.80
Poland	19	0.5	13	0.4	0.68
Other Countries	881	21.5	707	19.1	0.80
World total	4100	100	3700	100	0.90

A solution that has been meeting the above problems for some time, is using so-called green concrete to make concrete structures [42–48]. Structures made in this manner are environmentally sustainable concrete structures, which are characterized by their overall impact on the ecosystem of humans and animals being as limited as possible. It should be added that in case of such construction, a holistic approach to their design and implementation is used. The impact of buildings constructed in this way is assessed at all stages of operation, involving five phases. They are summarized and described in details in Table 2.

**Table 2.** Implementation phases in a complete cycle of a typical concrete structure [49,50].

Phase Number	Stage	Activities
Phase 1	Place of raw material acquisition	<ul style="list-style-type: none"> <li>• Extraction of raw materials,</li> <li>• production of components,</li> <li>• transport to concrete plant.</li> </ul>
Phase 2	Concrete plant	<ul style="list-style-type: none"> <li>• dosing of ingredients,</li> <li>• production of mix,</li> <li>• transport to construction site.</li> </ul>
Phase 3	Construction	<ul style="list-style-type: none"> <li>• laying the mix,</li> <li>• consolidation,</li> <li>• care of elements.</li> </ul>
Phase 4	Period of facility use	<ul style="list-style-type: none"> <li>• operation,</li> <li>• maintenance,</li> <li>• repairs and overhauls.</li> </ul>
Phase 5	“The second life of the structure”	<ul style="list-style-type: none"> <li>• demolition,</li> <li>• reuse,</li> <li>• recycling.</li> </ul>

It should therefore be noted that green concrete is not defined universally, however, when used to build the structure, it must meet the requirements for strength and durability, whereas its ingredients must be environmentally friendly materials (Table 2).

Therefore, in modern technology of green concrete, a great interest of scientists and practical engineers concerns the possibility of modifying the microstructure of cement-based materials by using chemically active mineral additives. These include natural pozzolans, siliceous and calcareous fly ash, silica fume, granulated blast furnace slag, lime powder, and other materials that replace the cement binder in the composition of the concrete mix, e.g., [51–69]. There is also the increasingly used potential of nanotechnology, in which green concrete nanoadditives are used included in its composition, such as e.g., nanosilica, carbon nanotubes, and active chemical nanoadditives, e.g., [70–73]. Both traditional concrete additives and nanoadditives that are part of modern cement matrix composites are referred to as supplementary cementitious materials (SCMs) [74–81].

The use of SCMs in the production of concrete composites promotes sustainability in the concrete industry [82]. However, due to the fact that in the vast majority of countries in the world, energy generated for industrial and domestic needs is still produced by burning hard coal, siliceous fly ash (FA), which is a by-product of these processes, is the main additive to ordinary and green concrete composites currently produced, e.g., [83–85]. This is evidenced, among other things, by the amount of these by-products generated annually at almost one billion tons [86,87]. Therefore, a serious issue becomes the FA management in such a way that they do not adversely affect the environment because, in some respects, they are hazardous materials, e.g., [88,89]. In addition, such measures result in a reduction of the basic binder used in the production of the concrete composites, i.e., the OPC, in the composition of the concrete mix. Consequently, this results in: lower costs of producing such materials [90], reduced consumption of thermal and electric energy [91] and, what is important, a marked reduction in emission of harmful GHG [92]. Considering the above aspects, it must be stated that the utilization of FA also carries an evident pro-ecological factor, e.g., [93–95].

Utilization of finely grained FA in green concrete technology brings considerable advantages, as demonstrated in many previous publications, e.g., [96,97]. Substitution of OPC by this material in an amount up to 20% contributes to the improvement of parameters of mature concrete composites, such as compressive and tensile strength [98,99], fracture toughness [100–102], heat resistance [103], abrasion and erosion resistance [104], resistance

to vibration and impact loads [105–108], and rheological properties of the material [109,110]. Substitution of OPC using FA also causes a reduction in the negative effects in structures made on the basis of such a binder due to the corrosive effects and expansion [111–113], electrical resistivity [114] and the dynamic loads [115–118].

However, the concept of green concrete is undergoing intensive development and is presenting more and more opportunities for the use of these sustainable materials in the concrete industry. One of the most effective solutions is the possibility of supplementation cement binder with several active modifiers at the same time. Such a solution allows both the use of more binder substitutes, and the possible use of a synergistic interaction of individual pozzolanic active mineral additives with each other. You can find works in the literature presenting promising test results of green concrete carried on cement binders with different content of additives, starting from the simplest—binary [119–122] by ternary [123–125], and ending with the most technologically advanced—quaternary [126–134], or even quinary [135].

Therefore, this article proposes a solution involving modification of the concrete material with the main mineral additive, i.e., FA and the two types of silica-based additives. Supplementing the composition of the binder in the composites were, therefore, traditional non-compacted silica fume (SF), and the resulting from the modern concept of what is nanotechnology—nanosilica (nS). A proposal for green concrete made on the basis of quaternary binders formulated into various proportions of the above mineral additions is one of the possibilities for effective reduction of CO<sub>2</sub> and a significant reduction in the carbon footprint created in the production of ordinary concrete [135,136].

## 2. CO<sub>2</sub> Emission in the OPC Production Process and Possibility of Its Reduction by Using Green Concrete Based on Quaternary Binders

The World cement production generates around 7% of total CO<sub>2</sub> emissions globally, e.g., [137]. This harmful gas is produced during the three following operations (Figure 1):

- 50% is generated by the decomposition of limestone,
- 40% is because of fossil fuel combustion,
- 10% is contributed due to raw material transportation as well as electricity generation.

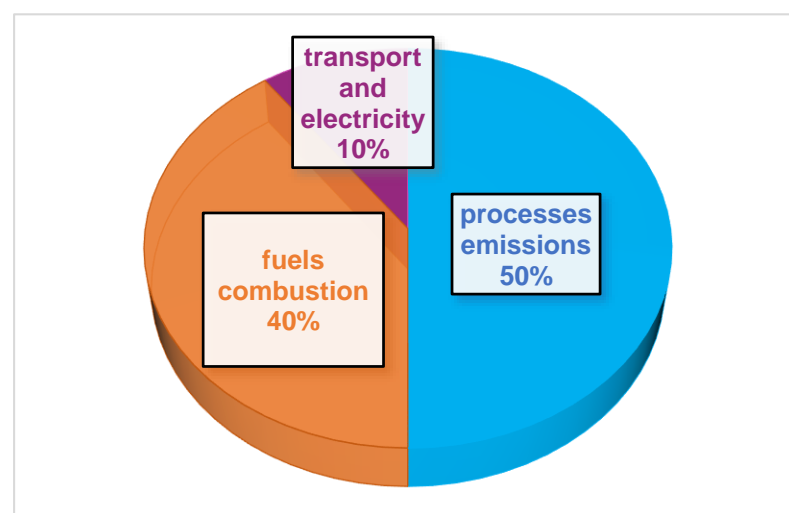


**Figure 1.** Operations in which CO<sub>2</sub> is generated in the OPC production process [49].

Generally, carbon dioxide in cement production processes is emitted from two basic direct sources, i.e., the process of decarbonization of calcium carbonate and fuel combustion, and two indirect sources, i.e., the production of electricity used in cement plants and transport.

The burning of Portland clinker and the subsequent production of OPC involves many complex technological operations. According to [49], Figure 2 provides a detailed diagram of these processes indicating the stages in which CO<sub>2</sub> emissions occurs.

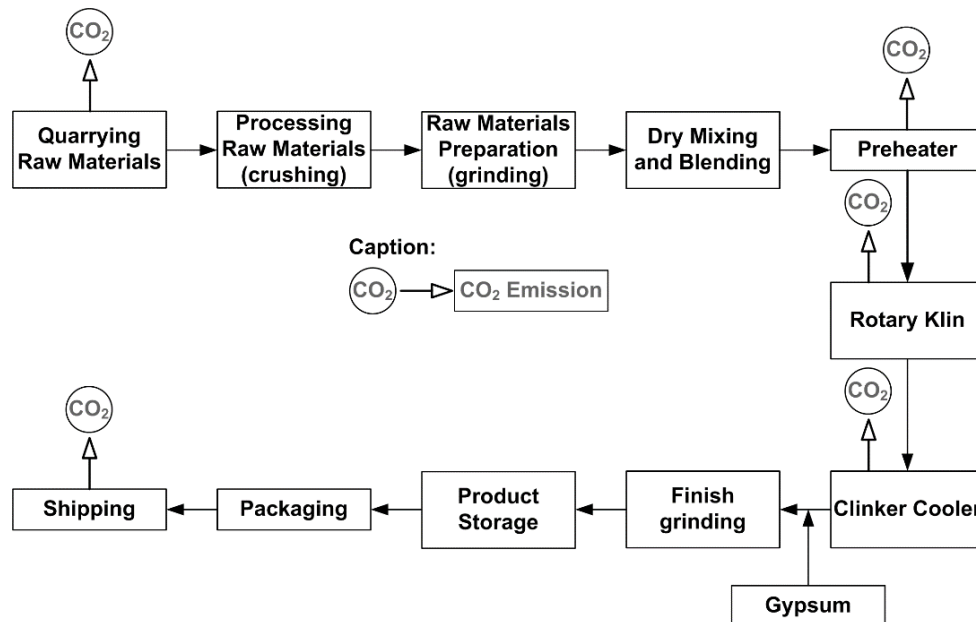


**Figure 2.** Detailed diagram showing the steps of OPC manufacturing and stages during which CO<sub>2</sub> is emitted [49].

The complex and multi-stage OPC production process causes that the production of one tonne of cement emits according to various sources from 0.8 to 1.0 tonne of CO<sub>2</sub> [138,139]. However, a simple relationship can be found between these processes when taking into account the so-called carbon footprint of concrete and all stages of cement production [140], i.e., 1 tonne of OPC  $\equiv$  1 tonne of CO<sub>2</sub> [141]. Based on this relationship and the data contained in Table 1, it can be concluded that currently, in global terms, approx. 4.1 billion tonnes of CO<sub>2</sub> is produced during the production of cement.

Therefore, the reduction of CO<sub>2</sub> emissions, generated during the burning of Portland clinker has been an important environmental problem for a long time. In this regard, more and more new research and theoretical simulations as well as novel implementation activities to reduce this negative effect are carried out, e.g., [142–145]. Their primary goal is to reduce as much CO<sub>2</sub> emission as possible, which is generated in OPC production at almost all stages (Figure 2). Therefore, there is an increasing development of modern binders based on the concepts of sustainable construction, e.g., [12–14,33,146–149].

One of such solutions is the possibility of partial replacement of the OPC with one or more together active mineral additives. Part of the materials used in this way, such as FA are troublesome industrial wastes. Hence, the benefits of such actions are multiplied, even turning into multiplicative relations.

As demonstrated in the following papers [150–158] the benefits associated with the implementation of substitutes for cement binder in the composition of the concrete mix are also related to their positive influence on the processes correlated with the formation of a compact structure in the concrete composites. Therefore, the following article presents a proposal for the use as a components of the green concrete of two pozzolanic active mineral additives, i.e., FA and SF in combination with nanoadditives, i.e., nS. Then, efforts were made to assess the benefits of such material modification, both for improved performance of composites analyzed and the possibility of reducing CO<sub>2</sub> emission.

Concretes made with applying the quaternary binder were tested for:

- their basic mechanical parameters analysis;

- changes that have occurred in their structure as a result of the substitution of cement binder by different compositions of supplements applied;
- reduction of harmful emissions of CO<sub>2</sub> by reducing the amount of OPC in the total weight of the binder used.

### 3. Experimental Section

#### 3.1. Materials

OPC 32.5 R as per EN 197-1:2011- Cement—Part 1 standard [159], class F FA, non-condensed SF, and Konasil K-200 nS in different proportion were used for the preparation of quaternary blends. It was also assumed that:

- the total amount of the binder in all composites will be constant;
- amount of the binder substitute at 10% and 5% will be constant for SF and nS, respectively;
- a variable parameter will be the addition of FA, which will replace the OPC in the amount of 0, 5, and 15%;
- the same water-binder ratio at level 0.4 in all mixtures.

Table 3 provides where all SCMs used came from.

**Table 3.** The origin of SCMs used.

Origin	Kind of SCMs			
	OPC	FA	SF	nS
Country		Poland		South Korea
City	Chełm	Puławy	Łaziska	Seul
Manufacturer	Cement Plant	Thermal-electric power station	Ironworks	OCI Chemical Company Ltd.

The chemical constituents of SCMs used are shown in Table 4, whereas the main physical properties of these materials were presented in Table 5. The XRF method supported by Epsilon 3× spectrometer (Malvern Panalytical, Malvern, UK) was used to evaluate the chemical composition of all binders, whereas laser granulometry using measuring device Masterizer 3000 and measuring range 0.01–3500 μm were used (Malvern Panalytical, Malvern, UK) to obtain average particle diameter of SCMs used.

**Table 4.** Chemical constituents of SCMs used.

Chemical	Component (wt %)			
	OPC	FA	SF	nS
SiO <sub>2</sub>	15.00	55.27	91.90	>99.8
Al <sub>2</sub> O <sub>3</sub>	2.78	26.72	0.71	-
Fe <sub>2</sub> O <sub>3</sub>	2.72	6.66	2.54	-
CaO	71.06	2.35	0.31	-
K <sub>2</sub> O	1.21	3.01	1.53	-
SO <sub>3</sub>	4.56	0.47	0.45	-
MgO	1.38	0.81	1.14	-
P <sub>2</sub> O <sub>5</sub>	-	1.92	0.63	-
TiO <sub>2</sub>	-	1.89	0.01	-
Ag <sub>2</sub> O	-	0.10	0.07	-
MnO	-	-	0.26	-
Cl	0.08	-	0.28	-

**Table 5.** Physical characteristics of SCMs used.

Physical Parameter	Kind of SCMs			
	OPC	FA	SF	nS
Specific gravity (g/cm <sup>3</sup> )	3.11	2.14	2.21	1.10
Blaine's fineness (m <sup>2</sup> /g)	0.33	0.36	1.40	200
Average particle diameter (μm)	40	30	11	0.012
Color (visually)	Light gray	Dark gray	Black	White

The proposed selection of components for the implementation of concretes was aimed at assessing the synergy of the interaction of individual additives with each other in the direction of improving the mechanical parameters and microstructure of composites. The control concrete (REF) did not contain any binder substitutes, while in the Q series concretes, efforts were made to determine the effect of FA on the analyzed parameters of concretes containing SF and nS with a constant content of these modifiers. For this purpose, the concrete of the Q1 series was, in a sense, a quasi-reference concrete, i.e., with 0% FA content, in relation to materials with the OPC substitute by FA at 5% and 15% respectively in the series of concretes Q2 and Q3.

Moreover, coarse aggregate (natural gravel 2–8 mm size with specific gravity 2.65 and compressive strength 34 MPa), fine aggregate (pit sand, maximum size 2.00 mm with specific gravity 2.60 and compressive strength 33 MPa), plasticizer, Basf Liquol BV-18, and the laboratory pipeline water for preparation all mixtures were used. Table 6 provides information on various mix proportions of SCMs with OPC for reference (REF) series (100% OPC), and quaternary binders (Q series) considered for the present study.

**Table 6.** Various mix proportions of OPC and SCMs used for the experimental work.

Mix	Type of Binders	Proportion of Binder Components (%)			
		OPC	FA	SF	nS
REF	Reference	100	–	–	–
Q	Quaternary				
Q1		85	0	10	5
Q2		80	5	10	5
Q3		70	15	10	5

### 3.2. Methods

Compressive strength ( $f_{cm}$ ) and splitting tensile strength ( $f_{ctm}$ ) of the hardened concrete as per standard procedure given in EN 12390-3: 2011+AC: 2012 [160] and EN 12390-6: 2009 [161] were measured. Standard concrete cubes of dimensions 150 × 150 × 150 mm<sup>3</sup> were prepared and tested in 300 T capacity (Walter + Bai ag, type NS19/PA1; Löhningen, Switzerland). The rate of loading was kept between 0.5 to 0.8 MPa/s. In order to ensure the repeatability of test results, six specimens for all composites and both mechanical tests were prepared and reported after 28 days of curing.

In addition to macroscopic examinations, structural analysis of all the composites was also carried out. SEM study was conducted to identify the morphological characteristics of the concrete mix prepared from quaternary binders. In the course of the micro-structural experiments, the following assumptions were made:

- the test specimens had rectangular shapes and approximate dimensions of 10 × 10 × 3 mm<sup>3</sup>;
- the test was conducted using a QUANTA FEG 250, which was equipped with an energy dispersive Spectroscopy (EDS EDAX);
- for each of the composites, the images were taken at the same magnifications, i.e., 8000 and 16,000 times and the same reference scales, i.e., 20, and 10 μm;
- for each type of material, the images were taken on six samples;

- 30 images were taken for each sample, from which representative images were selected;
- on the SEM images, the following were marked or described: areas with the FA grains, areas with clearly distinguishable phases, e.g., calcium silicate hydrate (C-S-H), calcium hydroxide (CH), or ettringite (E).

In addition to assessing strength parameters and microstructure in concretes modified with pozzolanic additives, the additional goal of the study was to determine the environmental benefits related to possible limitation of CO<sub>2</sub> emissions as a result of reducing the use of OPC in the composition of the concrete mixture and replacing this basic binder with useful mineral additives. Assuming that the annual OPC production is 4.1 million tonnes (Table 1), and considering the fact that production of 1 ton of the binder leaves CO<sub>2</sub> generated to atmosphere approximately in the same amount—as discussed in Section 2—attempts were made to estimate the limit that can be achieved in the emission of this oxide by the replacement of OPC with proposed SCMs in various formulations rates.

The possible reduction of CO<sub>2</sub> emissions, in the case of using concretes with the proposed compositions, was therefore obtained on the basis of the percentage reduction in the use of the OPC in each of the composites. Since the amount of OPC produced is practically equal to the amount of generated CO<sub>2</sub>—therefore, globally, the percentage reduction in OPC consumption will correspond to the same amount of reduction in CO<sub>2</sub> emissions.

## 4. Results and Discussion

### 4.1. Strength Parameters

Table 7 provides the main mechanical parameters with standard deviations ( $\delta$ ) of analyzed composites. In quaternary concrete Q2 and Q3, it was observed that both strengths of the concrete reduced with increased FA percentage level from 5 to 15%, which can be attributed to the properties of FA that suppress the heat of hydration of cement and, in turn, requires a longer curing period for pozzolanic reactions [47,149,150]. Nevertheless, concrete of Q2 series, i.e., with 5% FA additive, in combination with 10% of SF additive and 5% of nS additive had the best strength parameters. Equally good results of modification were observed in the Q1 concrete series, i.e., with the addition of SF and nS only. Definitely the lowest strength was recorded in the case of the reference concrete (Table 7). Therefore, it can be clearly stated that the OPC substitution by each proposed composition of active pozzolan mineral additives brings measurable benefits in the results of the basic mechanical properties of the quaternary green concrete.

**Table 7.** Compressive strength and splitting tensile strength of quaternary concretes.

Mix	Analysed Parameters (MPa)	
	$f_{cm} \pm \delta$	$f_{ctm} \pm \delta$
REF	38.32 ± 1.74	2.90 ± 0.24
Q1	53.89 ± 2.61	4.02 ± 0.30
Q2	56.77 ± 3.36	4.26 ± 0.35
Q3	50.12 ± 4.52	3.76 ± 0.42

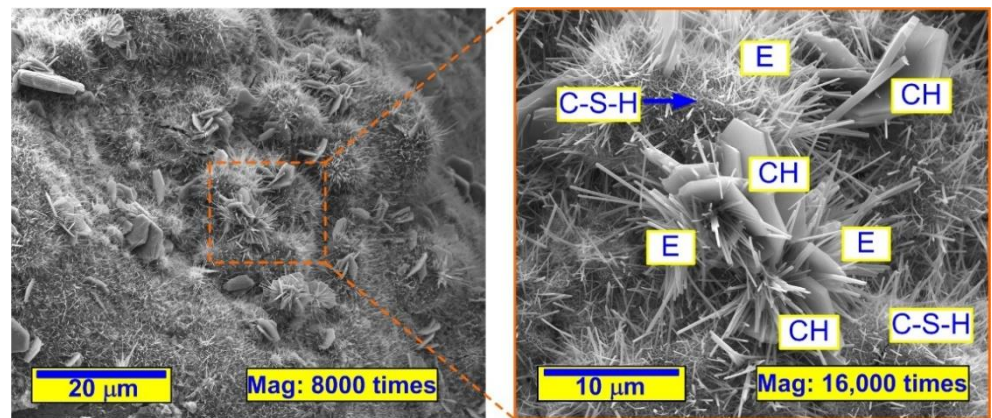
Analysis of convergence of the results obtained also allows to conclude that diversification of composition of the cement binder contributes to a slight increase in scatter of the obtained test results. The highest values of the standard deviation were observed for the Q3 series composite, i.e., at 30% substitution of the cement binder, and the smallest, on the other hand, in the reference concrete. Nevertheless, for every concrete, the level of variability in the results did not exceed 10%, which, however may indicate their convergence at an acceptable level, inclining to recognize the obtained average values of both strengths as fully reliable (Table 7). Satisfactory strength results obtained, both  $f_{cm}$  and  $f_{ctm}$  were tried

to be explained by the accurate assessment of individual composite structures using SEM technology.

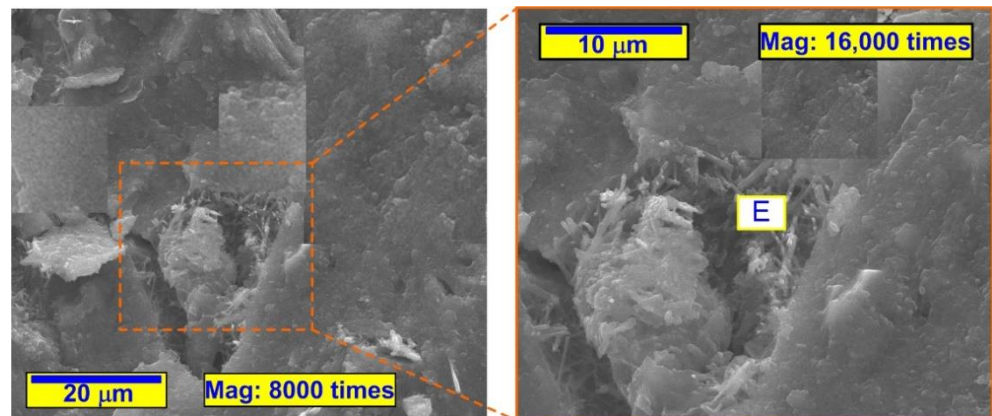
#### 4.2. SEM Studies

Figure 3 shows sample representative SEM images of the microstructures of all the green quaternary concretes analyzed after 28 days of curing. Additionally, descriptions of characteristic details observed in the structure of all materials are summarized in Table 8.

From the inspection of the SEM images, a clear influence of the SCMs used can be observed, which caused a faster and more dynamic development of the cement matrix structure. There was a rapid growth of dense C-S-H phase in all quaternary concretes (Figure 3b–d), whereas, in the reference concrete, the stage of nucleation of individual types of phases was still visible (Figure 3a). The lack of the addition of pozzolanic-active and fine-grained supplements of OPC caused a significant delay in the formation of a dense matrix in the reference concrete. The structure of this composite was somewhat delayed in time, taking into account the curing processes of slurry, compared to the effects visible in the Q series concretes.



(a)



(b)

Figure 3. Cont.

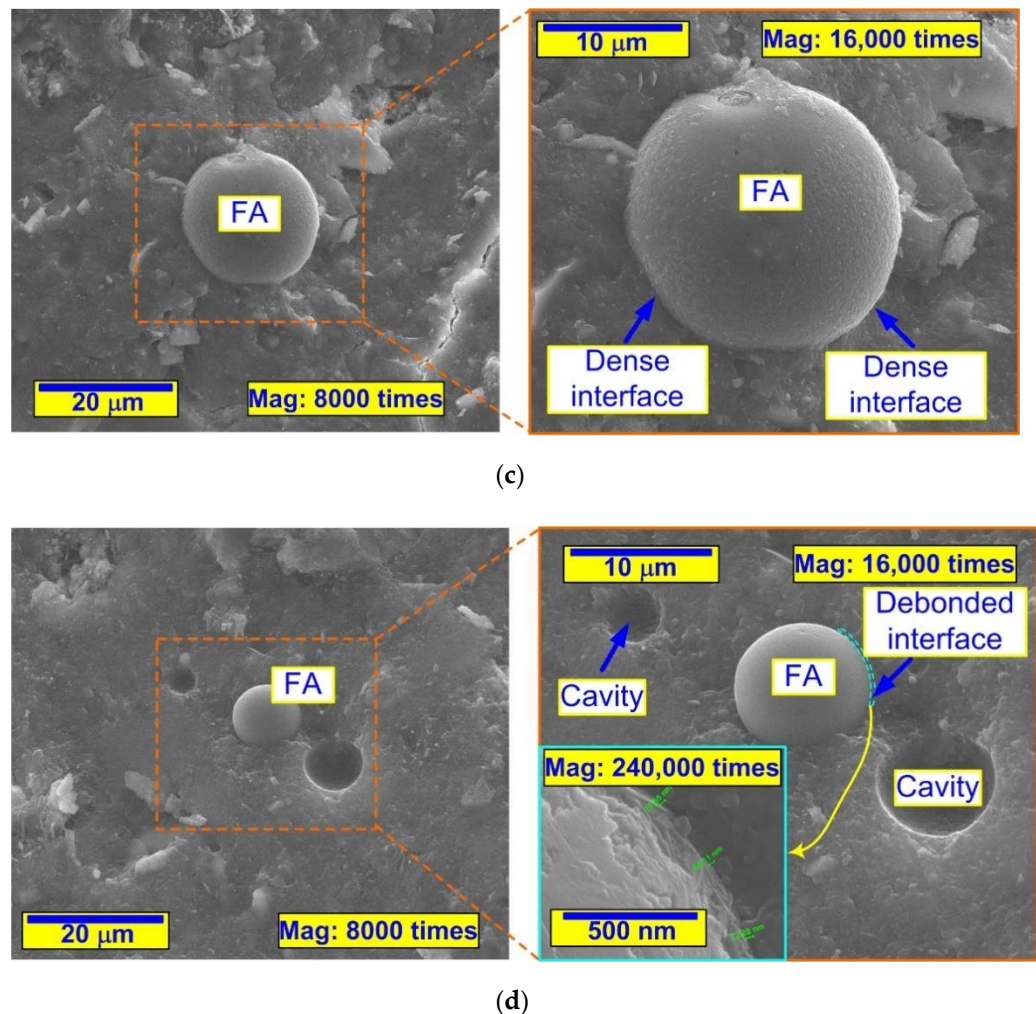


**Figure 3.** SEM micrographs of analyzed quaternary concretes including SCMs: (a) REF, (b) Q1, (c) Q2, (d) Q3; CH—calcium hydroxide, C-S-H—calcium silicate hydrate, E—ettringite, FA—fly ash.

In the quaternary concrete, with silica additives only, the structure contained a few porous places filled with ettringite phase products (Figure 3b). Composites containing FA were differed in structure, depending on the amount of waste used. In the concrete of the Q2 series, FA grains were well embedded in the matrix structure, and no visible damage was observed in the area of their contacts at the phase boundary. Concrete with a higher content of micro-filler, i.e., the Q3 series was characterized by a significantly worse morphology compared to the Q2 composite. A large amount of FA particles caused that they were not fully embedded in the structure of the matrix, and contained small microdamage in places of contact with the matrix. In numerous previous works, e.g., [98,155,157,162–164] it has been proven that a large amount of FA is not able to fully react during the formation of the matrix structure after 28 days of curing. The benefits of such a modification, however, are delayed with time. Thus, after a month, instead of strengthening it, one can, unfortunately, get the opposite effect.

This phenomenon, mentioned above, can be observed using magnification unprecedented for this type of material, i.e., 240,000 times. Thanks to this, it was possible to capture details and diagnosis of microcracks at the grain contact. One such magnification is presented in Figure 3d. In addition, in the concrete of the Q3 series numerous places with separated FA grains were observed. It can be concluded that the structure of this quaternary concrete presented in the SEM photographs is definitely the least favorable.

**Table 8.** Morphology of the matrix of analyzed quaternary concretes.

Mix	Morphological Characteristics of Cement Matrix (Based on Observations)
REF	<ul style="list-style-type: none"> <li>• the first stages of phase nucleation in the material structure;</li> <li>• formation of the first phases structures in the composite;</li> <li>• diversification of all basic phases, matrix structure appears disordered;</li> <li>• the beginnings of the formation of the structures of CSH phase;</li> <li>• visible structures of the CSH phase in the form of needles;</li> <li>• visible of portlandite crystals.</li> </ul>
Q1	<ul style="list-style-type: none"> <li>• compact structures of the cement matrix with visible of CSH phase;</li> <li>• few pores visible in the matrix structure;</li> <li>• visible needles of the ettringite phase;</li> <li>• formation of phase structures comprehensively covering large areas of the matrix;</li> <li>• matrix structure appears to be highly homogenized;</li> <li>• the matrix structure is cohesive.</li> </ul>
Q2	<ul style="list-style-type: none"> <li>• compact structures of CSH phase;</li> <li>• the FA particles are bonded to the matrix;</li> <li>• the FA grains clearly “immersed” in the matrix structure;</li> <li>• the FA grains are faintly visible as they are embedded into the matrix structure and react;</li> <li>• increasingly compacted the matrix structure is visible;</li> <li>• compact interfacial transition zone between the FA grains and matrix.</li> </ul>
Q3	<ul style="list-style-type: none"> <li>• compact structures of CSH phase;</li> <li>• small visible defects at the boundary of the FA grains;</li> <li>• areas and cavities of separation of the FA grains from the matrix structure are visible;</li> <li>• reactive FA grains are visible;</li> <li>• weakly compacted interfacial transition zone between the FA grains and matrix;</li> <li>• the FA grains with ambivalent contact structure at junction with the matrix.</li> </ul>

#### 4.3. Assessing of Environmental Benefits—CO<sub>2</sub> Reduction

In addition to the benefits of improved mechanical parameters and structure of concrete as a result of the proposed modifications using several mineral additives, an analysis of the environmental benefits that may result from such a solution was also carried out. Table 9 presents the values of limitations in CO<sub>2</sub> emission generated during OPC production when replacing the main binder with individual compositions of SCMs.

**Table 9.** Annual reduction of CO<sub>2</sub> emission in green quaternary concrete with SCMs.

Mix	Annual Reduction of CO <sub>2</sub> Emission (ton)
REF	0
Q1	615,000,000
Q2	820,000,000
Q3	1,230,000,000

As a consequence, the production of concretes in which OPC would be replaced in the concrete mix with the proposed additives in particular percentage ranges could allow the significant reduction of CO<sub>2</sub> emissions in the range from over 0.6 mln tons to over 1,200,000,000 tons (Table 9).

When analyzing Table 9, it is clearly visible that the resulting environmental benefits are directly related to the percentage of materials used. The biggest limitation of CO<sub>2</sub> emission was obtained in the case of the Q3 series concrete, where OPC was replaced

up to 30%. Reduction at the level of well over a million tonnes of CO<sub>2</sub> during the year is definitely not to be underestimated. In the case of the Q2 series composite, it will be possible to reduce CO<sub>2</sub> emission for nearly 1 million tons, when for the Q1 series concrete, only a little over 0.5 million tons.

## 5. Conclusions

The article presents the research results of basic mechanical properties and structures analysis of green concrete made on the basis of OPC and three pozzolanic active mineral additives. They were made using a basic additive currently used to modify the cement binder, i.e., FA, in two different proportions. In addition, non-compacted SF forms and modern nanoadditives in nS form were used. Research of mechanical parameters and microstructure of the subject composites were supported with environmental analyzes. The goal was to determine the tangible benefits of the applied modification of materials in the context of a possible limitation of CO<sub>2</sub> emission in the concrete industry, formed mainly in the process of Portland cement clinker burning out. (Figure 1). From the presented studies the following conclusions can be drawn:

- (1) OPC substitution by each proposed composition of active pozzolan mineral additives brings measurable benefits in the results of the basic strength parameters of quaternary green concrete. The best results were obtained using the synergy of all three substitutes of the cement binder in the proportions used in the concrete of the Q2 series.
- (2) The structure of the quaternary green concrete after 28 days of curing is characterized by a dense matrix. In the concrete of the Q1 series, porous places filled with transformation products of the ettringite phase were observed additionally. Concretes containing FA were characterized, however, by tight contacts in places of connection of grains with the matrix—in the case of a composite with a lower content of additive—and minor microdamage on the phase boundary, that were seen at a very high magnifications in the concrete with the addition 15% of FA.
- (3) A small percentage of FA additive has a positive effect on the structure of the matrix containing a fine-grained and very active composition of additives in the form of SF and nS. Unfortunately, increasing the content of FA in the binder composition to over a dozen percent causes a clear weakening of the composite structure based on the quaternary binder.
- (4) The structure of the reference concrete was disordered and has presented numerous phases during the process of their nucleation and transformation. This definitely translated into the weakest results of the mechanical parameters of this material.
- (5) The results of the composites' mechanical properties testing show the highest convergence in the reference concrete. As the quantity of additives in the composition of the cement binder increases, the level of scatter of results increases. Nevertheless, it takes satisfactory values in all quaternary green concretes.
- (6) Reducing the amount of OPC in the composition of the concrete mix in quaternary green concrete causes obvious environmental benefits associated with the significant reduction of CO<sub>2</sub> emission in the production of OPC from over 0.6 mln tons to over 1,200,000,000 tons.
- (7) Quaternary green concrete containing additives and nanoadditives could be a useful alternative to plain concretes covering both the technical and environmental aspects.

**Funding:** The research leading to these results has received funding from the MINIATURA 2 Grant, No. 2018/02/X/ST8/02726: funded by the National Science Center of Poland.

**Institutional Review Board Statement:** Not applicable.

**Informed Consent Statement:** Not applicable.

**Data Availability Statement:** No new data were created or analyzed in this study. Data sharing is not applicable to this article.

**Conflicts of Interest:** The author declares no conflict of interest.

## References

1. Sanjuan, M.A.; Estevez, E.; Argiz, C. Carbon dioxide absorption by blast-furnace slag mortars in function of the curing intensity. *Energies* **2019**, *12*, 2346. [[CrossRef](#)]
2. Zhang, H.; Liu, J.; Wu, B.; Zhang, Z. Axial compressive behaviour of geopolymer recycled lump concrete. *Materials* **2020**, *13*, 533. [[CrossRef](#)]
3. Rahman, A.; Rasul, M.G.; Khan, M.M.K.; Sharma, S. Impact of alternative fuels on the cement manufacturing plant performance: An overview. *Proc. Eng.* **2013**, *56*, 393–400. [[CrossRef](#)]
4. Zou, F.; Shen, K.; Hu, C.; Wang, F.; Yang, L.; Hu, S. Effect of sodium sulfate and C-S-H seeds on the reaction of fly ash with different amorphous alumina contents. *ACS Sustain. Chem. Eng.* **2020**, *8*, 1659–1670. [[CrossRef](#)]
5. Benehelal, E.; Zahedi, G.; Hashim, H. A novel design for green and economical cement manufacturing. *J. Clean. Prod.* **2012**, *22*, 60–66. [[CrossRef](#)]
6. Haw, T.T.; Hart, F.; Rashidi, A.; Pasbakhsh, P. Sustainable cementitious composites reinforced with metakaolin and halloysite nanotubes for construction and building applications. *Appl. Clay Sci.* **2020**, *188*, 105533. [[CrossRef](#)]
7. Afkhami, B.; Akbarian, B.; Beheshti, N.; Kakaee, A.H.; Shabani, B. Energy consumption assessment in a cement production plant. *Sustain. Energy Technol. Assess.* **2015**, *10*, 84–89. [[CrossRef](#)]
8. Madloul, N.A.; Saidur, R.; Hossain, M.S.; Rahim, N.A. A critical review on energy use and savings in the cement industries. *Renew. Sustain. Energy Rev.* **2011**, *15*, 2042–2060. [[CrossRef](#)]
9. Gielen, D.; Taylor, P. Indicators for industrial energy efficiency in India. *Energy* **2009**, *34*, 962–969. [[CrossRef](#)]
10. Atmaca, A.; Yumrutas, R. Analysis of the parameters effecting energy consumption of a rotary kiln in cement industry. *Appl. Therm. Eng.* **2014**, *66*, 435–444. [[CrossRef](#)]
11. Radwan, A.M. Different possible ways for saving energy in the cement production. *Adv. Appl. Sci. Res.* **2012**, *3*, 1162–1174.
12. Mikulcic, H.; Vujanovic, M.; Duic, N. Improving the sustainability of cement production by using numerical simulation of limestone thermal degradation and pulverized coal combustion in a cement calciner. *J. Clean. Prod.* **2015**, *88*, 262–271. [[CrossRef](#)]
13. Grillo Reno, M.L.; Ferrari Alves, L.F.; Escobar Palacio, J.C.; Souza, L.; Centeno González, F.O.; Pacheco Torres, P.J. Environmental analyze of cement production with application of wastes. *Engevista* **2017**, *19*, 916–930. [[CrossRef](#)]
14. Long, G.; Gao, Y.; Xie, Y. Designing more sustainable and greener self-compacting concrete. *Constr. Build. Mater.* **2015**, *84*, 301–306. [[CrossRef](#)]
15. Mikulcic, H.; Vujanovic, M.; Duic, N. Reducing the CO<sub>2</sub> emissions in Croatian cement industry. *Appl. Energy Prod.* **2013**, *101*, 41–48. [[CrossRef](#)]
16. Mikulcic, H.; Vujanovic, M.; Markovska, N.; Filkoski, R.V.; Ban, M.; Duic, N. CO<sub>2</sub> emission reduction in the cement industry. *Chem. Eng. Trans.* **2013**, *35*, 703–708.
17. Ali, M.B.; Saidur, R.; Hossain, M.S. A review on emission analysis in cement industries. *Renew. Sustain. Energy Rev.* **2011**, *15*, 2252–2261. [[CrossRef](#)]
18. Jahromy, S.S.; Azam, M.; Jordan, C.; Harasek, M.; Winter, F. The potential use of fly ash from the pulp and paper industry as thermochemical energy and CO<sub>2</sub> storage material. *Energies* **2021**, *14*, 3348. [[CrossRef](#)]
19. Voldsund, M.; Gardarsdottir, S.O.; Lena, E.D.; Pérez-Calvo, J.-F.; Jamali, A.; Berstad, D.; Fu, C.; Romano, M.; Roussanaly, S.; Anantharaman, R.; et al. Comparison of technologies for CO<sub>2</sub> capture from cement production—Part 1: Technical evaluation. *Energies* **2019**, *12*, 559. [[CrossRef](#)]
20. Gardarsdottir, S.O.; Lena, E.D.; Romano, M.; Roussanaly, S.; Voldsund, M.; Pérez-Calvo, J.-F.; Berstad, D.; Fu, C.; Anantharaman, R.; Sutter, D.; et al. Comparison of technologies for CO<sub>2</sub> capture from cement production—Part 2: Cost analysis. *Energies* **2019**, *12*, 542. [[CrossRef](#)]
21. Cao, C.; Liu, H.; Hou, Z.; Mehmood, F.; Liao, J.; Feng, W. A review of CO<sub>2</sub> storage in view of safety and cost-effectiveness. *Energies* **2020**, *13*, 600. [[CrossRef](#)]
22. Sadowski, T.; Golewski, G.L. A failure analysis of concrete composites incorporating fly ash during torsional loading. *Compos. Struct.* **2018**, *183*, 527–535. [[CrossRef](#)]
23. Kovacic, J.; Marsavina, L.; Linul, E. Poisson's ratio of closed-cell aluminum foams. *Materials* **2018**, *11*, 1904. [[CrossRef](#)]
24. Raheel, M.; Rahman, F.; Ali, Q. A stoichiometric approach to find optimum amount of fly ash needed in cement concrete. *SN Appl. Sci.* **2020**, *2*, 1100. [[CrossRef](#)]
25. Kang, S.-H.; Kwon, Y.-H.; Moon, J. Quantitative analysis of CO<sub>2</sub> uptake and mechanical properties of air lime-based materials. *Energies* **2019**, *12*, 2903. [[CrossRef](#)]
26. Golewski, G.L.; Gil, D.M. Studies of fracture toughness in concretes containing fly ash and silica fume in the first 28 days of curing. *Materials* **2021**, *14*, 319. [[CrossRef](#)] [[PubMed](#)]
27. Chajec, A. Granite powder vs. fly ash for the sustainable production of air-cured cementitious mortars. *Materials* **2021**, *14*, 1208. [[CrossRef](#)]

28. Miraldo, S.; Lopes, S.; Pcheco-Torgal, F.; Lopes, A. Advantages and shortcomings of the utilization of recycled wastes as aggregates in structural concretes. *Constr. Build. Mater.* **2021**, *298*, 123729. [[CrossRef](#)]
29. Golewski, G.L. Determination of fracture toughness in concretes containing siliceous fly ash during mode III loading. *Struct. Eng. Mech.* **2017**, *62*, 1–9. [[CrossRef](#)]
30. Golewski, G.L. Effect of fly ash addition on the fracture toughness of plain concrete at third model of fracture. *J. Civ. Eng. Manag.* **2017**, *23*, 613–620. [[CrossRef](#)]
31. Pacheco-Torgal, F. High tech startup creation for energy efficient built environment. *Ren. Sust. Ener. Rev.* **2017**, *71*, 618–629. [[CrossRef](#)]
32. Deja, J.; Uliasz-Bochenczyk, A.; Mokrzycki, E. CO<sub>2</sub> emissions from Polish cement industry. *Int. J. Greenh. Gas. Control.* **2010**, *4*, 583–588. [[CrossRef](#)]
33. Ali, N.; Jaffar, A.; Anwer, M.; Khan, S.; Anjum, M.N.; Hussain, A.; Raja, M.; Ming, X. The greenhouse gas emissions produced by cement production and its impact on environment: A review of global cement processing. *Int. J. Res.* **2015**, *2*, 488–500.
34. Benehelal, E.; Zahedi, G.; Shamsaei, E.; Bahadori, A. Global strategies and potentials to curb CO<sub>2</sub> emissions in cement industry. *J. Clean. Prod.* **2013**, *51*, 142–161. [[CrossRef](#)]
35. Gil, D.M.; Golewski, G.L. Potential of siliceous fly ash and silica fume as a substitute of binder in cementitious concrete. *E3S Web Conf.* **2018**, *49*, 00030. [[CrossRef](#)]
36. Gil, D.M.; Golewski, G.L. Effect of silica fume and siliceous fly ash addition on the fracture toughness of plain concrete in mode I. *IOP Conf. Ser. Mater. Sci. Eng.* **2018**, *416*, 012065. [[CrossRef](#)]
37. Gursel, A.P.; Maryman, H.; Ostertag, C. A life-cycle approach to environmental, mechanical, and durability properties of “green” concrete mixes with rice husk ash. *J. Clean. Prod.* **2016**, *112*, 823–836. [[CrossRef](#)]
38. Meyer, C. The greening of the concrete industry. *Cem. Concr. Compos.* **2009**, *31*, 601–605. [[CrossRef](#)]
39. Imbabi, M.S.; Carrigan, C.; McKenna, S. Trends and development in green cement and concrete technology. *Int. J. Sust. Bui. Environ.* **2012**, *1*, 194–216. [[CrossRef](#)]
40. Al-Mansour, A.; Chow, C.L.; Feo, L.; Penna, R.; Lau, D. Green concrete: By-products utilization and advanced approaches. *Sustainability* **2019**, *11*, 5145. [[CrossRef](#)]
41. USGS. Mineral Commodity Summaries, 2001, 2011, 2020; U.S. Geological Survey: Reston, VA, USA. Available online: <https://www.usgs.gov/centers/nmic/mineral-commodity-summaries> (accessed on 18 February 2020).
42. Golewski, G.L. Validation of the favorable quantity of fly ash in concrete and analysis of crack propagation and its length—Using the crack tip tracking (CTT) method—In the fracture toughness examinations under Mode II, through digital image correlation. *Constr. Build. Mater.* **2021**, *296*, 122362. [[CrossRef](#)]
43. Barnat-Hunek, D.; Grzegorzczak-Frańczak, M.; Szymańska-Chargot, M.; Łagód, G. Effect of eco-friendly cellulose nanocrystals on physical properties of cement mortars. *Polymers* **2019**, *11*, 2088. [[CrossRef](#)]
44. Thenepalili, T.; Ngoc, N.T.M.; Tuán, L.; Son, T.H.; Hieu, H.H.; Thuy, D.T.N.; Thao, N.T.T.; Tam, D.T.T.; Huyen, N.; Van, T.T.; et al. Technological solutions for recycling ash slag from the Cao Ngan Coal Power Plant in Vietnam. *Energies* **2018**, *11*, 2018. [[CrossRef](#)]
45. Vishwakarma, V.; Ramachandran, D. Green concrete mix using solid waste and nanoparticles as alternatives—A review. *Constr. Build. Mater.* **2018**, *162*, 96–103. [[CrossRef](#)]
46. Golewski, G.L. Evaluation of fracture processes under shear with the use of DIC technique in fly ash concrete and accurate measurement of crack path lengths with the use of a new crack tip tracking method. *Measurement* **2021**, *181*, 109632. [[CrossRef](#)]
47. Rahimireskati, S.; Ghabraie, K.; Garcez, E.O.; Al-Ameri, R. Improving sorptivity and electrical resistivity of concrete utilizing biomedical polymeric waste sourced from dialysis treatment. *Int. J. Sus. Eng.* **2021**. [[CrossRef](#)]
48. Szlag, M. Evaluation of cracking patterns in cement composites—From basics to advances: A review. *Materials* **2020**, *13*, 2490. [[CrossRef](#)] [[PubMed](#)]
49. Huntzinger, D.N.; Eatmon, T.D. A life-cycle assessment of Portland cement manufacturing: Comparing the traditional process with alternative technologies. *J. Clean. Prod.* **2009**, *17*, 668–675. [[CrossRef](#)]
50. Glavind, M. *Guidelines for Green Concrete Structures*; fib Bulletin 67; Guide to good practice; International Federation for Structural Concrete (fib): Lusanne, Switzerland, 2012.
51. Suchorab, Z.; Franus, M.; Barnat-Hunek, D. Properties of fibrous concrete made with plastic fibers from E-Waste. *Materials* **2020**, *13*, 2414. [[CrossRef](#)] [[PubMed](#)]
52. Szcześniak, A.; Zychowicz, J.; Stolarski, A. Influence of fly ash additive on the properties of concrete with slag cement. *Materials* **2020**, *13*, 3265. [[CrossRef](#)] [[PubMed](#)]
53. Mehri Khansari, N.; Fakoor, M.; Berto, F. Probabilistic micromechanical damage model for mixed mode I/II fracture investigation of composite materials. *Theor. Appl. Fract. Mech.* **2019**, *99*, 177–193. [[CrossRef](#)]
54. Golewski, G.L. Effect of curing time on the fracture toughness of fly ash concrete composites. *Compos. Struct.* **2018**, *185*, 105–112. [[CrossRef](#)]
55. Golewski, G.L.; Sadowski, T. A study of mode III fracture toughness in young and mature concrete with fly ash additive. *Solid State Phenom.* **2016**, *254*, 120–125. [[CrossRef](#)]
56. Khaji, Z.; Fakoor, M. Strain energy release rate in combination with reinforcement isotropic solid model (SERIS): A new mixed-mode I/II criterion to investigate fracture behavior of orthotropic materials. *Theor. Appl. Fract. Mech.* **2021**, *113*, 102962. [[CrossRef](#)]

57. Ji, G.; Peng, X.; Wang, S.; Hu, C.; Ran, P.; Sun, K.; Zeng, L. Influence of magnesium slag as a mineral admixture on the performance of concrete. *Constr. Build. Mater.* **2021**, *295*, 123619. [[CrossRef](#)]
58. Figala, P.; Drochytka, R.; Cerny, V.; Kolisko, J. Structure of polymer-cement composite optimized with secondary raw materials. *Mater. Struct. Tech.* **2018**, *1*, 26–31. [[CrossRef](#)]
59. Chen, Y.-G.; Guan, L.-L.; Zhu, A.-Y.; Chen, W.-J. Foamed concrete containing fly ash: Properties and application to backfilling. *Constr. Build. Mater.* **2021**, *273*, 121685. [[CrossRef](#)]
60. Golewski, G.L. Generalized fracture toughness and compressive strength of sustainable concrete including low calcium fly ash. *Materials* **2017**, *10*, 1393. [[CrossRef](#)]
61. Li, H.; Sun, H.; Tian, J.; Yang, Q.; Wan, Q. Mechanical and ultrasonic testing of self-compacting concrete. *Energies* **2019**, *12*, 2187. [[CrossRef](#)]
62. Li, H.; Sun, H.; Zhang, W.; Gou, H.; Yang, Q. Study on mechanical properties of self-compacting concrete and its filled in-line multi-cavity steel tube bundle shear wall. *Energies* **2019**, *12*, 3466. [[CrossRef](#)]
63. Abolhasani, A.; Nazarpour, H.; Dehestani, M. Effects of silicate impurities on fracture behavior and microstructure of calcium aluminate cement concrete. *Eng. Fract. Mech.* **2021**, *242*, 107446. [[CrossRef](#)]
64. Fakoor, M.; Rafiee, R.; Zare, S. Equivalent reinforcement isotropic model for fracture investigation of orthotropic materials. *Steel Compos. Struct.* **2019**, *30*, 1–12.
65. Berto, F.; Ayatollahi, M.; Marsavina, L. Mixed Mode Fracture. *Theoret. Appl. Fract. Mech.* **2017**, *91*, 1. [[CrossRef](#)]
66. Lata, P.; Kaur, I.; Singh, K. Transversely isotropic thin circular plate with multi-dual-phase lag heat transfer. *Steel Compos. Struct.* **2020**, *35*, 343–351.
67. Lata, P.; Kaur, I. Thermomechanical interactions in transversely isotropic magneto thermoelastic solid with two temperatures and without Energy dissipation. *Steel Compos. Struct.* **2019**, *32*, 779–793.
68. Shill, S.K.; Al-Deen, S.; Ashraf, M.; Hutchison, W.; Hossain, M.M. Performance of amine cured epoxy and silica fume modified cement mortar under military airbase operating conditions. *Constr. Build. Mater.* **2020**, *232*, 117280. [[CrossRef](#)]
69. Shill, S.K.; Al-Deen, S.; Ashraf, M.; Hutchison, W. Resistance of fly ash based geopolymer mortar to both chemicals and high thermal cycles simultaneously. *Constr. Build. Mater.* **2020**, *239*, 117886. [[CrossRef](#)]
70. Zhang, P.; Han, S.; Golewski, G.L.; Wang, X. Nanoparticle-reinforced building materials with applications in civil engineering. *Adv. Mech. Eng.* **2020**, *12*, 1–4. [[CrossRef](#)]
71. Szeląg, M. Development of cracking patterns in modified cement matrix with microsilica. *Materials* **2018**, *11*, 1928. [[CrossRef](#)]
72. Szostak, B.; Golewski, G.L. Effect of nano admixture of CSH on selected strength parameters of concrete including fly ash. *IOP Conf. Ser. Mater. Sci. Eng.* **2018**, *416*, 012105. [[CrossRef](#)]
73. Szostak, B.; Golewski, G.L. Improvement of strength parameters of cement matrix with the addition of siliceous fly ash by using nanometric C-S-H seeds. *Energies* **2020**, *13*, 6734. [[CrossRef](#)]
74. Lothenbach, B.; Scrivener, K.; Hooton, R.D. Supplementary cementitious materials. *Cem. Concr. Res.* **2011**, *41*, 1244–1256. [[CrossRef](#)]
75. Snellings, R.; Martens, G.; Elsen, J. Supplementary cementitious materials. *Rev. Miner. Geochem.* **2012**, *74*, 211–278. [[CrossRef](#)]
76. Booya, E.; Gorospe, K.; Ghaedena, H.; Das, S. Durability properties of engineered pulp fibre reinforced concretes made with and without supplementary cementitious materials. *Compos. B Eng.* **2019**, *172*, 376–386. [[CrossRef](#)]
77. Luhar, S.; Cheng, T.-W.; Luhar, I. Incorporation of natural waste from agricultural and aquacultural farming as Supplementary Materials with green concrete: A review. *Compos. B Eng.* **2019**, *175*, 107076. [[CrossRef](#)]
78. Pacewska, B.; Wilińska, I. Usage of supplementary cementitious materials: Advantages and limitations. Part I. C-S-H, C-A-S-H and other products formed in different binding mixtures. *J. Therm. Anal. Cal.* **2020**, *142*, 371–393. [[CrossRef](#)]
79. Xie, T.; Yang, G.; Zhao, X.; Xu, J.; Fang, C. A unified model for predicting the compressive strength of recycled aggregate concrete containing supplementary cementitious materials. *J. Clean. Prod.* **2020**, *251*, 119752. [[CrossRef](#)]
80. Duchesne, J. Alternative supplementary cementitious materials for sustainable concrete structures: A review on characterization and properties. *Waste Biomass Valorization* **2021**, *12*, 1219–1236. [[CrossRef](#)]
81. Yang, K.-H.; Jung, Y.-B.; Cho, M.-S.; Tae, S.-H. Effect of supplementary cementitious materials on reduction of CO<sub>2</sub> emission from concrete. *J. Clean. Prod.* **2016**, *112*, 4041–4052.
82. Hossain, M.U.; Poon, C.S.; Dong, Y.H.; Xuan, D. Evaluation of environmental impact distribution methods for supplementary cementitious materials. *Renew. Sustain. Energy Rev.* **2018**, *82*, 597–608. [[CrossRef](#)]
83. Golewski, G.L.; Sadowski, T. Experimental investigation and numerical modeling fracture processes in fly ash concrete at early age. *Solid State Phenom.* **2012**, *188*, 158–163. [[CrossRef](#)]
84. Wang, X.; Gao, M.; Wang, M.; Wu, C. Chloride removal from municipal solid waste incineration fly ash using lactic acid fermentation broth. *Waste Manag.* **2021**, *130*, 23–29. [[CrossRef](#)]
85. Hemalatha, T.; Ramaswamy, A. A review on fly ash characteristics—Towards promoting high volume utilization in developing sustainable concrete. *J. Clean. Prod.* **2017**, *147*, 546–559. [[CrossRef](#)]
86. Golewski, G.L. The influence of microcrack width on the mechanical parameters in concrete with the addition of fly ash: Consideration of technological and ecological benefits. *Constr. Build. Mater.* **2019**, *197*, 849–861. [[CrossRef](#)]
87. Belviso, C. State-of-the-art applications of fly ash from coal and biomass: A focus on zeolite synthesis processes and issues. *Progr. Ener. Combust. Sci.* **2018**, *65*, 109–135. [[CrossRef](#)]

88. Golewski, G.L. Studies of natural radioactivity of concrete with siliceous fly ash addition. *Cem. Wapno Beton* **2015**, *2*, 106–114.
89. Deng, S.; Shu, Y.; Li, S.; Tian, G.; Huang, J.; Zhang, F. Chemical forms of the fluorine, chlorine, oxygen and carbon in coal fly ash and their correlations with mercury retention. *J. Hazard. Mater.* **2016**, *301*, 400–406. [[CrossRef](#)]
90. Ikponmwosa, E.E.; Ehikhuenmen, S.O.; Irene, K.K. Comparative study and empirical modelling of pulverized coconut shell, periwinkle shell and palm kernel shell as a pozzolans in concrete. *Acta Polytech.* **2019**, *59*, 560–572. [[CrossRef](#)]
91. Golewski, G.L. Energy savings associated with the use of fly ash and nanoadditives in the cement composition. *Energies* **2020**, *13*, 2184. [[CrossRef](#)]
92. Barnat-Hunek, D.; Grzegorzczak-Frańczak, M.; Klimek, B.; Pavlikova, M.; Pavlik, Z. Properties of multi-layer renders with fly ash and boiler slag admixtures for salt-laden masonry. *Constr. Build. Mater.* **2021**, *278*, 122366. [[CrossRef](#)]
93. Mousavi, S.R.; Afshoon, I.; Bayatpour, M.A.; Davarpanah, A.; Mahmoud Miri, T.Q. Effect of waste glass and curing aging on fracture toughness of self-compacting mortars using ENDB specimen. *Constr. Build. Mater.* **2021**, *282*, 122711. [[CrossRef](#)]
94. Rahmani, E.; Sharbatdar, M.K.; Beygi, M.H.A. Influence of cement contents on the fracture parameters of Roller compacted concrete pavement (RCCP). *Constr. Build. Mater.* **2021**, *289*, 123159. [[CrossRef](#)]
95. Golewski, G.L.; Sadowski, T. Macroscopic evaluation of fracture processes in fly ash concrete. *Solid State Phenom.* **2016**, *254*, 188–193. [[CrossRef](#)]
96. Golewski, G.L. Green concrete composite incorporating fly ash with high strength and fracture toughness. *J. Clean. Prod.* **2018**, *172*, 218–226. [[CrossRef](#)]
97. Golewski, G.L. Improvement of fracture toughness of green concrete as a result of addition of coal fly ash. Characterization of fly ash microstructure. *Mater. Charact.* **2017**, *134*, 335–346. [[CrossRef](#)]
98. Dragas, J.; Tomic, N.; Ignatovic, S.; Marinkovic, S. Mechanical and time-dependent properties of high-volume fly ash concrete for structural use. *Mag. Concr. Res.* **2016**, *68*, 632–645. [[CrossRef](#)]
99. Kosior-Kazberuk, M.; Lelusz, M. Strength development of concrete with fly ash addition. *J. Civ. Eng. Manag.* **2007**, *13*, 115–122. [[CrossRef](#)]
100. Golewski, G.L. An analysis of fracture toughness in concrete with fly ash addition, considering all models of cracking. *IOP Conf. Ser. Mater. Sci. Eng.* **2018**, *416*, 012029. [[CrossRef](#)]
101. Golewski, G.L.; Sadowski, T. The fracture toughness the  $K_{IIC}$  of concretes with fly ash (FA) additive. *Constr. Build. Mater.* **2017**, *143*, 444–454. [[CrossRef](#)]
102. Golewski, G.L. Changes in the fracture toughness under mode II loading of low calcium fly ash (LCFA) concrete depending on ages. *Materials* **2020**, *13*, 5241. [[CrossRef](#)] [[PubMed](#)]
103. Nadeem, A.; Memon, S.A.; Lo, T.Y. The performance of fly ash and metakaolin concrete at elevated temperatures. *Constr. Build. Mater.* **2014**, *62*, 67–76. [[CrossRef](#)]
104. Cai, X.; He, Z.; Tang, S.; Chen, X. Abrasion erosion characteristics of concrete made with moderate heat Portland cement, fly ash and silica fume using sandblasting test. *Constr. Build. Mater.* **2016**, *127*, 804–814. [[CrossRef](#)]
105. Golewski, G.L. A new principles for implementation and operation of foundations for machines: A review of recent advances. *Struct. Eng. Mech.* **2019**, *71*, 317–327.
106. Golewski, G.L. On the special construction and materials conditions reducing the negative impact of vibrations on concrete structures. *Mater. Today. Procs.* **2021**, *45*, 4344–4348. [[CrossRef](#)]
107. Park, S.; Beak, J.; Kim, K.; Park, Y.-J. Study on reduction effect of vibration propagation due to internal explosion using composite materials. *Int. J. Concr. Struct. Mater.* **2021**, *15*, 30. [[CrossRef](#)]
108. Craciun, E.M. Energy criteria for crack propagation in prestresses elastic composites. *Sol. Mech. Appl.* **2008**, *154*, 193–237.
109. Szostak, B.; Golewski, G.L. Rheology of cement pastes with siliceous fly ash and the C-S-H nano-admixture. *Materials* **2021**, *14*, 3640. [[CrossRef](#)]
110. Hu, X.; Shi, C.; Shi, Z.; Tong, B.; Wang, D. Early age shrinkage and heat of hydration of cement-fly ash-slag ternary blends. *Constr. Build. Mater.* **2017**, *153*, 857–865. [[CrossRef](#)]
111. Chindapasirt, P.; Rukzon, S. Strength, porosity and corrosion resistance of ternary blend Portland cement, rice husk ash and fly ash mortar. *Constr. Build. Mater.* **2008**, *22*, 1601–1606. [[CrossRef](#)]
112. Golewski, G.L.; Sadowski, T. An analysis of shear fracture toughness toughness  $K_{IIC}$  and microstructure in concretes containing fly-ash. *Constr. Build. Mater.* **2014**, *51*, 207–214. [[CrossRef](#)]
113. Joshaghani, A. The effect of trass and fly ash in minimizing alkali-carbonate reaction in concrete. *Constr. Build. Mater.* **2017**, *150*, 583–590. [[CrossRef](#)]
114. Jingjing, L.; Fusheng, Z.; Long, X.; Bo, K.; Xiaohui, T.; Yongfeng, D.; Chengbin, Y. Mechanisms of stabilized/solidified heavy metal contaminated soils with cement-fly ash based on electrical resistivity measurements. *Measurement* **2019**, *141*, 85–94.
115. Golewski, G.L. A novel specific requirements for materials used in reinforced concrete composites subjected to dynamic loads. *Compos. Struct.* **2019**, *223*, 110939. [[CrossRef](#)]
116. Golewski, G.L. Physical characteristics of concrete, essential in design of fracture-resistant, dynamically loaded reinforced concrete structures. *Mater. Des. Proc. Comm.* **2019**, *1*, e82. [[CrossRef](#)]
117. Mehdizadeh, M.; Maghshenas, A.; Khosnari, M.M. On the effect of internal friction on torsional and axial cyclic loading. *Inter. J. Fat.* **2021**, *145*, 106113. [[CrossRef](#)]

118. Golewski, G.L. The beneficial effect of the addition of fly ash on reduction of the size of microcracks in the ITZ of concrete composites under dynamic loading. *Energies* **2021**, *14*, 668. [[CrossRef](#)]
119. Biricik, H.; Sarier, N. Comparative study of the characteristics of nanosilica-, silica fume- and fly ash-incorporated cement mortars. *Mater. Res.* **2014**, *17*, 570–582. [[CrossRef](#)]
120. Karim, M.R.; Zain, M.F.M.; Jamil, M.; Lai, F.C. Development of a zero-cement binder using slag, fly ash, and rice husk ash with chemical activator. *Adv. Mater. Sci. Eng.* **2015**, *2015*, 247065. [[CrossRef](#)]
121. Golewski, G.; Sadowski, T. Fracture toughness at shear (mode II) of concretes made of natural and broken aggregates. *Brittle Matrix Compos.* **2006**, *8*, 537–546.
122. Patel, N.; Dave, R.; Modi, S.; Joshi, C.; Vora, S.; Solanki, M. Effect of binary and quaternary blends on compressive strength. *Int. J. Civ. Eng. Technol.* **2016**, *7*, 242–246.
123. El-Chabib, H.; Ibrahim, A. The performance of high-strength flowable concrete made with binary, ternary, or quaternary binder in hot climate. *Constr. Build. Mater.* **2013**, *47*, 245–253. [[CrossRef](#)]
124. Manju, R.; Premalatha, J. Binary, ternary and quaternary effect of pozzolanic binders and filler materials on the properties of self compacting concrete (SCC). *Int. J. Adv. Eng. Technol.* **2016**, *7*, 674–683.
125. Chinnaraju, K.; Subramanian, K.; Senthil Kumar, S.R.R. Strength properties of HPC using binary, ternary and quaternary cementitious blends. *Struct. Concr.* **2010**, *11*, 191–198. [[CrossRef](#)]
126. More, S.; Londhe, R.S. Experimental analysis of quaternary cement binder. *Recent Trends Civ. Eng. Technol.* **2020**, *10*, 12–17.
127. Pipilikaki, P.; Katsioti, M. Study of the hydration process of quaternary blended cements and durability of the produced mortars and concretes. *Constr. Build. Mater.* **2009**, *23*, 2246–2250. [[CrossRef](#)]
128. Dave, N.; Misra, A.K.; Srivastava, A.; Sharma, A.K.; Kaushik, S.K. Study on quaternary micro-structure, strength, durability considering the influence of multi-factors. *Constr. Build. Mater.* **2017**, *139*, 447–457. [[CrossRef](#)]
129. Dave, N.; Misra, A.K.; Srivastava, A.; Kaushik, S.K. Setting time and standard consistency of quaternary binders: The influence of cementitious material addition and mixing. *Int. J. Sustain. Built Environ.* **2017**, *6*, 30–36. [[CrossRef](#)]
130. Dave, N.; Misra, A.K.; Srivastava, A.; Kaushik, S.K. Experimental analysis of strength and durability properties of quaternary cement binder and mortar. *Constr. Build. Mater.* **2016**, *107*, 117–124. [[CrossRef](#)]
131. Dave, N.; Misra, A.K.; Srivastava, A.; Sharma, A.K.; Kaushik, S.K. Green quaternary concrete composites: Characterization and evaluation of the mechanical properties. *Struct. Concr.* **2018**, *19*, 1280–1289. [[CrossRef](#)]
132. Dhrangadharia, S.; Vishwakarma, S.; Kumar, A.; Saran, B. Effect of quaternary binders systems on mechanical properties of concrete. *Int. J. Eng. Sci. Res.* **2018**, *6*, 1–10.
133. Manju, R.; Premalatha, J. Binary, ternary and quaternary effect of fillers on fresh and hardened properties of self compacting concrete (SCC). *Int. J. Adv. Inf. Sci. Technol.* **2014**, *21*, 12–19.
134. Bassuoni, M.T.; Nehdi, M.L. Resistance of self-consolidating concrete of sulfuric acid attack with consecutive pH reduction. *Cem. Concr. Res.* **2007**, *37*, 1070–1084. [[CrossRef](#)]
135. Papatzani, S.; Paine, K. Optimization of low-carbon footprint quaternary and quinary (37% fly ash) cementitious nanocomposites with polycarboxylate or aqueous nanosilica particles. *Adv. Mater. Sci. Eng.* **2019**, *2019*, 5931306. [[CrossRef](#)]
136. Chen, Y.; Ng, S.T.; Hossain, M.U. Approach to establish carbon emission benchmarking for construction materials. *Car. Manag.* **2019**, *9*, 1–18. [[CrossRef](#)]
137. Keun-Hyeok, Y. Assessment of CO<sub>2</sub> reduction of alkali-activated concrete. *J. Clean. Prod.* **2013**, *39*, 265–272.
138. Mehta, P.K. Reducing the environmental impact of concrete. *Concr. Inter.* **2001**, *23*, 61–66.
139. Mehta, P.K. Greening of the concrete industry for sustainable development. *Concr. Inter.* **2002**, *24*, 23–28.
140. Habert, G.; Billard, C.; Rossi, P.; Chen, C.; Roussel, N. Cement production technology improvement compared to factor 4 objectives. *Cem. Concr. Res.* **2010**, *40*, 820–826. [[CrossRef](#)]
141. Rathish Kumar, P.; Sumanth Reddy, C.; Saleem Baig, M. Compressive strength performance of high strength concretes using binary supplementary cementitious materials. *Cem. Wapno Beton* **2014**, *1*, 8–16.
142. Warguła, Ł.; Kukla, M.; Lijewski, P.; Dobrzyński, M.; Markiewicz, F. Influence of innovative woodchipper speed control systems on exhaust gas emissions and fuel consumption in urban areas. *Energies* **2020**, *13*, 3330. [[CrossRef](#)]
143. Shimizu, O.; Nagai, S.; Fujita, T.; Fujimoto, H. Potential for CO<sub>2</sub> reduction by dynamic wireless power transfer for passenger vehicles in Japan. *Energies* **2020**, *13*, 3342. [[CrossRef](#)]
144. Sanjuan, M.A.; Argiz, C.; Mora, P.; Zaragoza, A. Carbon dioxide uptake in the roadmap 2050 of the Spanish cement industry. *Energies* **2020**, *13*, 3452. [[CrossRef](#)]
145. Miller, S.A.; Horvath, A.; Monteiro, P.J.M.; Ostertag, C.P. Greenhouse gas emissions from concrete can be reduced by using mix proportions, geometric aspects, and age as design factors. *Environ. Res. Lett.* **2015**, *10*, 114017. [[CrossRef](#)]
146. Mikulcic, H.; Vujanovic, M.; Fidaros, D.K.; Priesching, P.; Minic, I.; Tatschl, R.; Duic, N.; Stefanovic, G. The application of CFD modelling to support the reduction of CO<sub>2</sub> emissions in cement industry. *Energy* **2012**, *45*, 264–473. [[CrossRef](#)]
147. Mikulcic, H.; Klemes, J.J.; Vujanovic, M.; Urbaniec, K.; Duic, N. Reducing greenhouse gasses emissions by fostering the deployment of alternative raw materials and energy sources in the cleaner cement manufacturing process. *J. Clean. Prod.* **2016**, *136*, 119–132. [[CrossRef](#)]
148. Golewski, G.L. An assessment of microcracks in the Interfacial Transition Zone of durable concrete composites with fly ash additives. *Compos. Struct.* **2018**, *200*, 515–520. [[CrossRef](#)]

149. Jin, R.; Chen, Q.; Soboyejo, A. Survey of the current status of sustainable concrete production in the U.S. *Res. Conser. Recyc.* **2015**, *105*, 148–159. [[CrossRef](#)]
150. Kurdowski, W. *Cement and Concrete Chemistry*; Springer: Dordrecht, The Netherlands; New York, NY, USA, 2014.
151. Beddu, S.; Ahmad, M.; Mohamad, D.; bin Noorul Ameen, M.I.; Itam, Z.; Mohd Kamal, N.L.; Nadiah Basri, N.A. Utilization of fly ash cenosphere to study mechanical and thermal properties of lightweight concrete. *AIMS Mater. Sci.* **2020**, *7*, 911–925. [[CrossRef](#)]
152. Beaudoin, J.J. Comparison of mechanical properties of compacted calcium hydroxide and Portland cement paste systems. *Cem. Concr. Res.* **1983**, *13*, 319–324. [[CrossRef](#)]
153. Beaudoin, J.J.; Gu, P.; Myers, R.E. The fracture of C-S-H and C-S-H/CH mixtures. *Cem. Concr. Res.* **1998**, *28*, 341–347. [[CrossRef](#)]
154. Golewski, G.L. Measurement of fracture mechanics parameters of concrete containing fly ash thanks to use of Digital Image Correlation (DIC) method. *Measurement* **2019**, *135*, 96–105. [[CrossRef](#)]
155. Zhang, M.H. Microstructure, crack propagation, and mechanical properties of cement pastes containing high volumes of fly ashes. *Cem. Concr. Res.* **1995**, *25*, 1165–1178. [[CrossRef](#)]
156. Golewski, G.L. Evaluation of morphology and size of cracks of the Interfacial Transition Zone (ITZ) in concrete containing fly ash (FA). *J. Hazard. Mater.* **2018**, *357*, 298–304. [[CrossRef](#)] [[PubMed](#)]
157. Papadakis, V.G. Effect of fly ash of Portland cement systems. Part I. Low-calcium fly ash. *Cem. Concr. Res.* **1999**, *29*, 1727–1736. [[CrossRef](#)]
158. Siddique, R. Effect of fine aggregate replacement with Class F fly ash on the mechanical properties of concrete. *Cem. Concr. Res.* **2003**, *33*, 539–547. [[CrossRef](#)]
159. EN 197-1:2011. *Cement—Part 1: Composition, Specifications and Conformity Criteria for Common Cements*; NSAI Standard: Dublin, Ireland, 2011.
160. EN 12390-3: 2011+AC: 2012. *Testing Hardened Concrete—Part. 3: Compressive Strength of Test Specimens*; British Standards Institution (BSI): London, UK, 2012.
161. EN 12390-6: 2009. *Testing Hardened Concrete—Part 6: Tensile Splitting Strength of Test Specimens*; British Standards Institution (BSI): London, UK, 2009.
162. Golewski, G.L. Estimation of the optimum content of fly ash in concrete composite based on the analysis of fracture toughness tests using various measuring systems. *Constr. Build. Mater.* **2019**, *213*, 142–155. [[CrossRef](#)]
163. Fraay, A.L.A.; Bijen, J.M.; de Haan, Y.M. The reaction of fly ash in concrete. A critical examination. *Cem. Concr. Res.* **1989**, *19*, 235–246. [[CrossRef](#)]
164. Odler, I. Strength of cement (final report). *Mater. Struct.* **1991**, *24*, 143–157. [[CrossRef](#)]